

# A Fast XPS study of propene decomposition over clean and sulphated Pt{111}

Adam F. Lee<sup>a\*</sup>, Karen Wilson<sup>b</sup>, Andrea Goldoni<sup>c</sup>, Rosanna Larciprete<sup>c</sup>, and Silvano Lizzit<sup>c</sup>

<sup>a</sup> Department of Chemistry, University of Hull, Hull HU6 7RX, UK.

<sup>b</sup> Department of Chemistry, University of York, York YO10 5DD, UK.

<sup>c</sup> Sincrotrone Trieste, Trieste, Italy.

Received 11 September 2001; accepted 22 November 2001

The thermal decomposition of propene over clean and sulphate precovered Pt{111} has been followed by Fast XPS. The saturation propene coverage over the clean surface is 0.21 mL at 90 K. Propene is stable up to 200 K, above which molecular desorption and dehydrogenation result in the formation of a stable propylidyne intermediate adlayer at 300 K. Propylidyne decomposes above 400 K eventually forming graphitic carbon above 800 K. Preadsorbed surface sulphate promotes room temperature propene combustion associated with the decomposition of a thermally unstable alkyl–sulphate complex. Propylidyne also forms as on clean Pt{111}, but is less reactive, its decomposition above 450 K triggering partial oxidation with residual surface oxygen to liberate gas phase CO.

**KEY WORDS:** X-ray photoelectron spectroscopy; catalysis; surface chemical reaction; alkenes

## 1. Introduction

The importance of hydrocarbon chemistry over catalytically active transition metal surfaces can hardly be overestimated, with contributions ranging from pollution control to fine chemicals synthesis. Consequently the chemisorption of hydrocarbons [1], and in particular of alkenes [2], on model single-crystal surfaces has been extensively investigated. In the case of ethylene on Pt{111}, both the initial adsorption geometry and formation of an ethylidyne dehydrogenation intermediate have been identified [3–5]. Higher (C<sub>3</sub>–C<sub>5</sub>) alkenes are also postulated to decompose via corresponding alkylidyne intermediates [6–7]; however such interconversions have never been directly monitored. The rational design of improved catalysts requires new *in situ* analytical techniques that can quantify coexisting hydrocarbon surface species. We have recently shown it is possible to obtain time-resolved information about the thermal evolution of a reacting alkyne adlayer using Fast XPS [8]. This technique is complementary to vibrational spectroscopy in following the dynamics of the principal carbon environments [9].

Here Fast XPS is extended to the decomposition and oxidation of propene on Pt{111}. The nature and stability of the resulting intermediates are extremely important for Pt/Al<sub>2</sub>O<sub>3</sub> automotive emission control systems, wherein propene is a major component of the exhaust gases. We have recently shown that surface sulphoxy species can profoundly influence hydrocarbon

oxidation over platinum surfaces [10–12]. Sulphate enhances low temperature C–H bond activation, reducing the light-off temperature for propane and propene combustion over both single-crystal [10] and dispersed Pt [13]. However, little is known about the kinetics and efficiency of propene decomposition over clean platinum, or the nature of the sulphate–alkene interaction. This paper reports the thermal decomposition and oxidation of propene over clean and sulphate-promoted Pt{111}. We identify a new alkyl–sulphate complex responsible for low temperature CO<sub>2</sub> formation. The kinetics and efficiency of propene dehydrogenation via a stable propylidyne intermediate are also determined.

## 2. Experimental

Measurements were carried out at the SuperESCA beamline of the ELETTRA synchrotron radiation source using a Pt{111} single-crystal sample prepared by standard procedures and maintained under ultra high vacuum ( $\sim 1 \times 10^{-10}$  Torr). Quoted exposures are given in Langmuirs (1 L =  $1 \times 10^{-6}$  Torr s<sup>-1</sup>) and are uncorrected for ion-gauge sensitivity. The crystal was held at 90 K during dosing. Temperature programmed reaction data were acquired by application of a linear heating ramp ( $\sim 0.4$  K s<sup>-1</sup>) to the exposed sample. Propene (Air Liquide 99%), oxygen (MG 99%) and sulphur dioxide (Aldrich 98%) were used without purification. Sample dosing was performed by backfilling the vacuum chamber.

Carbon 1s and sulphur 2p XP spectra, referenced to the Fermi level, were acquired at a photon energy of

\* To whom correspondence should be addressed.  
E-mail: A.F.Lee@hull.ac.uk

400 eV and energy resolution of  $\sim$ 100 meV. Individual spectra were acquired approximately every 30 s during fast XP measurements. The background-subtracted spectra were fitted using a Doniach–Sunjic function convoluted with a Gaussian. Fitting parameters for molecular propene were determined from the low temperature uptake, while a common lineshape derived from graphitic carbon was adopted for the decomposition products. Sulphur peak assignments are taken from ref. [14]. Photoelectron spectra were measured using a 96-channel double-pass hemispherical analyser. Absolute carbon and sulphate coverages were determined by calibration with CO and H<sub>2</sub>S.

### 3. Results and discussion

#### 3.1. Propene decomposition

Figure 1 follows the thermal decomposition of a saturation propene adlayer ( $\theta = 0.21$  mL) on a clean Pt{111} surface during continuous heating. At 100 K a broad C 1s state centred around 283.6 eV is characteristic of molecular propene [15]; the peak shape reflects contributions from both the three inequivalent C environments and the vibrational fine structure [16]. A second higher binding energy state at  $\sim$ 284.6 eV corresponds to multilayer propene. Temperatures above 100 K desorb multilayer propene leaving the chemisorbed monolayer intact. This monolayer is stable up to  $\sim$ 200 K, above which  $\sim$ 33% of the propene desorbs molecularly in a continuous process extending up to  $\sim$ 250 K. Leading-edge analysis gives a desorption activation energy  $\Delta E_{\text{des}} = 58 \pm 3 \text{ kJ mol}^{-1}$ . Completion of this desorption coincides with a progressive sharpening and shifting of the C 1s spectra towards higher binding energy yielding a

single, narrow peak at 284.2 eV by 300 K. At this temperature it is generally accepted from TDS [5,17,18] and vibrational measurements [19,20] that the remaining adsorbed propene dehydrogenates *via* the loss of one hydrogen atom to form surface propylidyne ( $\text{Pt}_3\equiv\text{C}-\text{CH}_2-\text{CH}_3$ ). This peak shift and narrowing corresponds to the first direct observation of propene decomposition to propylidyne. This dehydrogenation, which requires free Pt sites, does not occur until sufficient propene has desorbed molecularly. Peak fitting shows that propylidyne formation is 100% efficient allowing the propylidyne binding energy to be pinpointed at 284.2 eV. The 0.5 eV chemical shift between propene and propylidyne likely reflects changes to both the terminal aliphatic carbon, during the proposed 1,2-sigmatropic hydrogen shifts in which a  $\mu^3$  surface geometry is adopted [21], and the allowed molecular vibrations. A leading-edge analysis of the fitted propylidyne intensity in figure 3 yields an apparent activation energy  $\Delta E_{\text{C}-\text{H}}^1 = 75 \pm 3 \text{ kJ mol}^{-1}$  with first-order kinetics. This validates prior indirect estimates from TDS [5] and SSIMS [22] which range from 73 to 83 kJ mol<sup>-1</sup>.

Above 400 K propylidyne decomposes in a series of dehydrogenation steps which liberate a variety of C<sub>x</sub>H<sub>y</sub> fragments. These give rise to a broad but weak C 1s signal spanning 283.5–284.5 eV. The inset to figure 1 shows the peak maximum also moves to lower binding energy with increasing temperature, presumably reflecting C–C cleavage and the formation of CH<sup>x</sup> species. Although initial breakdown is rapid, proceeding with  $\Delta E_{\text{C}-\text{H}}^2 = 113 \pm 3 \text{ kJ mol}^{-1}$ , significant propylidyne remains up to  $\sim$ 600 K. Higher temperatures result in the total dehydrogenation of residual CH<sub>x</sub> species [5,18], and indeed above 790 K we observe a well-defined surface carbon moiety with a binding energy  $\sim$ 283.5 eV. This new carbon state reflects graphite formation [7].

#### 3.2. Sulphate-mediated propene oxidation

The influence of surface sulphate on the chemistry of propene over Pt{111} was subsequently investigated. A

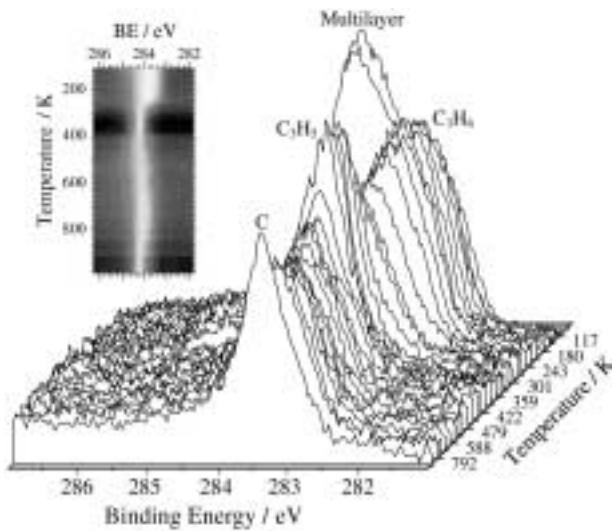


Figure 1. C 1s Fast XP temperature-programmed reaction spectra for a saturation C<sub>3</sub>H<sub>6</sub> adlayer on Pt{111}. Inset shows an image map highlighting peak shifts and transition temperatures.

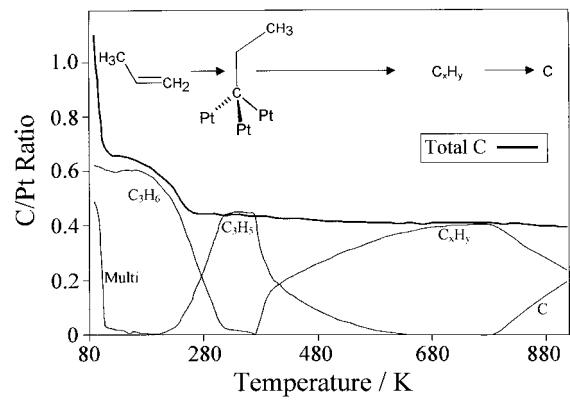


Figure 2. Deconvoluted C 1s components as a function of temperature for a saturation C<sub>3</sub>H<sub>6</sub> adlayer on Pt{111}. The total integrated C signal is also shown.

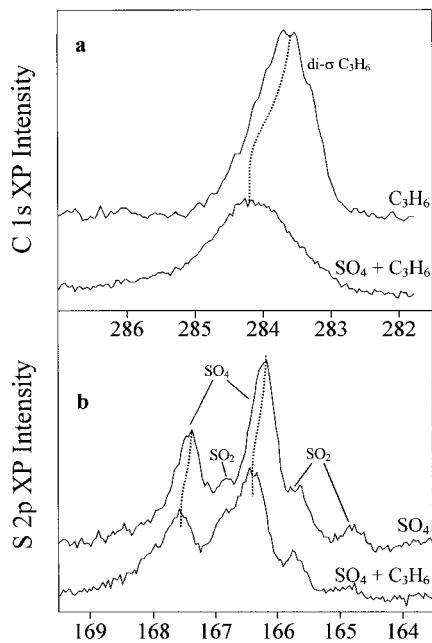


Figure 3. (a) C 1s XP spectra of 1 L  $\text{C}_3\text{H}_6$  on clean and  $\text{SO}_4$ -precovered  $\text{Pt}\{111\}$  and (b) S 2p XP spectra of  $\text{SO}_4$ -precovered  $\text{Pt}\{111\}$  before and after exposure to 1 L  $\text{C}_3\text{H}_6$ . All spectra recorded at 100 K.

sulphated surface was first prepared by adsorbing 12 L of  $\text{SO}_2$  onto oxygen presaturated  $\text{Pt}\{111\}$  at 100 K, and subsequently annealing to room temperature as described previously [10]. The resulting saturation sulphate coverage was 0.1 mL. Propene adsorption was then followed by XPS at 100 K. Carbon 1s spectra for 1 L propene on clean and sulphate precovered Pt are compared in figure 3(a), which reveals a significant peak broadening towards higher binding energy ( $\sim 0.55$  eV) in the presence of sulphate. Peak deconvolution (not shown here) shows a major new hydrocarbon state centred around 287 eV and a small amount of molecular propene in a 2:1 ratio. The corresponding S 2p spectra reveal propene adsorption likewise perturbs surface sulphate (figure 3(b)), increasing the  $\text{SO}_4$  binding energy by 0.2 eV and attenuating the overall S signal. This mutual perturbation provides evidence for a direct interaction between the two surface species which may form an alkyl–sulphate complex. The saturation propene coverage remains about 0.22 mL, confirming that preadsorbed sulphate does not act as an inert site-blocker.

The thermal evolution of this hydrocarbon adlayer was followed by Fast XPS (figure 4). The new high binding energy hydrocarbon state is relatively unstable, and  $\sim 50\%$  undergoes a gradual transformation to molecular propene on annealing to 180 K. Peak deconvolution (figure 5) shows no desorption occurs over this temperature range. This direct conversion suggests the perturbed state must retain a significant propyl character, again consistent with alkyl–sulphate formation. Above 180 K this alkyl moiety continues to decompose, now liberating

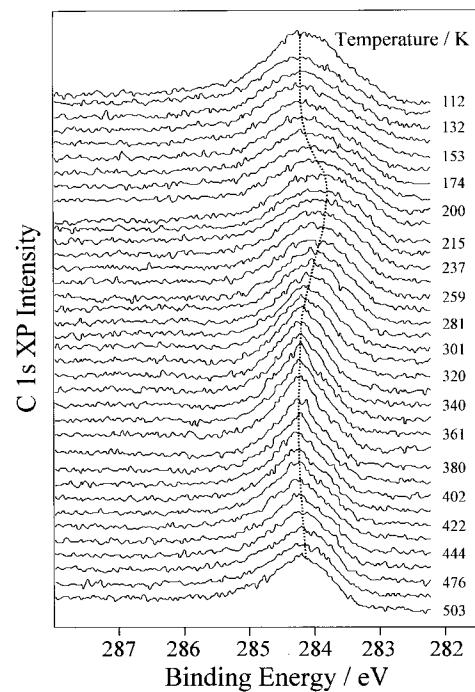


Figure 4. C 1s Fast XP temperature-programmed reaction spectra for 1 L  $\text{C}_3\text{H}_6$  adsorbed on  $\text{SO}_4$ -precovered  $\text{Pt}\{111\}$ .

reactive carbon-containing species which desorb from the surface. Simultaneously the S 2p spectra (not shown) show the reduction of  $\text{SO}_4$  to lower sulphoxy species and atomic sulphur. This breakdown continues more rapidly above 250 K and is accompanied by the same propene  $\rightarrow$  propylidyne observed over clean  $\text{Pt}\{111\}$ . About 20% of the total surface carbon desorbs between 220 and 320 K coincident with the appearance of gas-phase  $\text{CO}_2$  and  $\text{SO}_2$  (figure 6), strong evidence for decomposition of our postulated alkyl–sulphate complex. This is clearly illustrated by the correspondence between the peak minimum in the derivative total C 1s intensity and the  $\text{CO}_2$  (44 amu) desorption peak maximum. The initial total surface C:O ratio is  $\sim 5:3$ , this

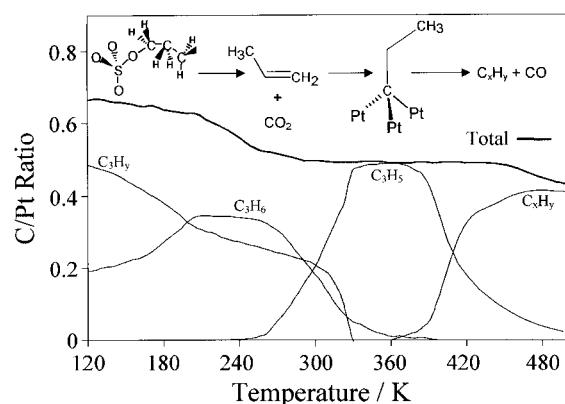


Figure 5. Deconvoluted C 1s components as a function of temperature for 1 L  $\text{C}_3\text{H}_6$  adsorbed on  $\text{SO}_4$ -precovered  $\text{Pt}\{111\}$ . The total integrated C signal is also shown.

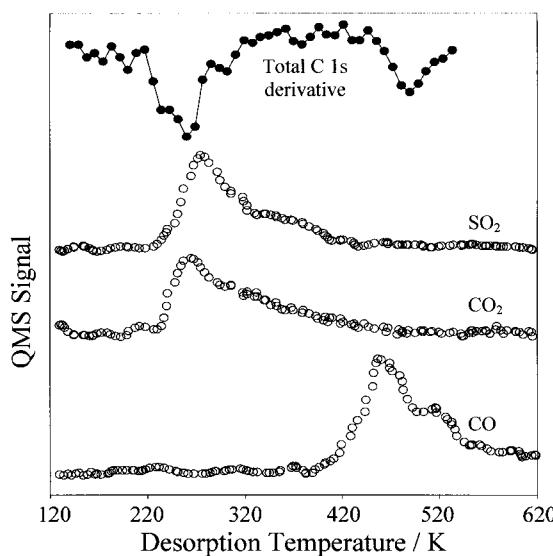


Figure 6. Temperature-programmed mass spectrometer reaction spectra for 1 L  $\text{C}_3\text{H}_6$  adsorbed on  $\text{SO}_4$ -precovered Pt[111]. The corresponding derivative total C 1s XP intensity is shown for comparison.

translates to a maximum  $\text{CO}_2$  yield of 0.2 mL and corresponding 30% decrease in the total carbon signal, consistent with the 25% drop observed in figure 5. Higher temperatures result in similar behaviour to that for the clean surface, with propylidyne decomposing via  $\text{CH}_x$  intermediates to liberate graphitic carbon. One notable difference is the small loss of surface carbon above 450 K, corresponding to CO desorption (figure 6), a process utilising the residual surface oxygen from  $\text{SO}_4$  breakdown.

#### 4. Conclusions

High resolution Fast XPS permits the direct observation of complex metal-catalysed hydrocarbon interconversion reactions. The activation barrier and threshold temperature for propene dehydrogenation to propylidyne have been determined and the first binding energy of a pure propylidyne adlayer measured. Propylidyne is thermally stable over a relatively narrow temperature regime and decomposes to graphitic carbon above 400 K via multiple intermediate hydrocarbon fragments. Surface sulphate reacts with propene at low temperatures

to form a metastable complex. This complex decomposes to liberate  $\text{CO}_2$  and  $\text{SO}_2$  at room temperature. Oxidation of molecular propene is hindered by the thermal stability of propylidyne, which decomposes above 450 K resulting in CO desorption.

#### Acknowledgment

Financial support by the UK Engineering and Physical Sciences Research Council under grant GR/M20877 is gratefully acknowledged.

#### References

- [1] F. Zaera, Chem. Rev. 95 (1995) 2651.
- [2] N. Sheppard and C. De la Cruz, Adv. Catal. 41 (1996) 1.
- [3] H. Ibach and S. Lehwald, J. Vac. Sci. Tech. 15 (1978) 407.
- [4] R.J. Koestner, M.A. Van-Hove and G.A. Somorjai, J. Phys. Chem. 87 (1983) 203.
- [5] M. Salmeron and G.A. Somorjai, J. Phys. Chem. 86 (1982) 341.
- [6] N.R. Avery and N. Sheppard, Proc. Roy. Soc. Lond. A405 (1986) 1.
- [7] R.J. Koestner, J.C. Frost, P.C. Stair, M.A. Vanhove and G.A. Somorjai, Surf. Sci. 116 (1982) 85.
- [8] A.F. Lee, K. Wilson, R.L. Middleton, A. Baraldi, A. Goldoni, G. Paolucci and R.M. Lambert, J. Am. Chem. Soc. 121 (1999) 7969.
- [9] A.F. Lee, K. Wilson, R.M. Lambert, A. Goldoni, A. Baraldi and G. Paolucci, J. Phys. Chem. B 104 (2000) 11729.
- [10] K. Wilson, C. Hardacre and R.M. Lambert, J. Phys. Chem. 99 (1995), 13755.
- [11] K. Wilson, A.F. Lee, C. Hardacre and R.M. Lambert, J. Phys. Chem. B. 102 (1998) 1736.
- [12] A.F. Lee, K. Wilson, R.M. Lambert, C.P. Hubbard, R.G. Hurley, R.W. McCabe and H.S. Ghandi, J. Catal. 184 (1999) 491.
- [13] H.C. Yao, H.K. Stephan and H.S. Ghandi, J. Catal. 67 (1981) 231.
- [14] M. Polcik, L. Wilde, J. Haase, B. Brena, G. Comelli and G. Paolucci, Surf. Sci. 381 (1997) L568.
- [15] E. Janin, S. Ringler, J. Weissenrieder, T. Åkermark, U.O. Karlsson, M. Göthelid, D. Nordlund and H. Ogasawara, Surf. Sci. 482 (2001) 83.
- [16] L.J. Sæthre, O. Sværøen, S. Svensson, S. Osborne, T.D. Thomas, J. Jauhainen and S. Aksela, Phys. Rev. A 55 (1997) 2748.
- [17] Y.-L. Tsai, C. Xu and B.E. Koel, Surf. Sci. 385 (1997) 37.
- [18] F. Zaera and D. Chrysostomou, Surf. Sci. 457 (2000) 89.
- [19] F. Zaera and D. Chrysostomou, Surf. Sci. 457 (2000) 71.
- [20] P.S. Cremer, X. Su, Y. Ron Shen and G.A. Somorjai, J. Phys. Chem. 100 (1996) 16302.
- [21] A.B. Anderson, D.B. Kang and Y. Kim, J. Am. Chem. Soc. 106 (1984) 6597.
- [22] K.M. Ogle, J.R. Creighton, S. Akhter and J.M. White, Surf. Sci. 169 (1986) 246.